



AFRL-OSR-VA-TR-2014-0122

---

## ATOMIC-SCALE PRINCIPLES OF COMBUSTION NANOCATALYSIS

Uzi Landman  
GEORGIA TECH RESEARCH CORPORATION

---

05/19/2014  
Final Report

DISTRIBUTION A: Distribution approved for public release.

Air Force Research Laboratory  
AF Office Of Scientific Research (AFOSR)/ RTE  
Arlington, Virginia 22203  
Air Force Materiel Command

<b>REPORT DOCUMENTATION PAGE</b>				<i>Form Approved</i> <b>OMB No. 0704-0188</b>	
Public reporting burden for this collection of information is estimated to average 1 hour per response, including the time for reviewing instructions, searching existing data sources, gathering and maintaining the data needed, and completing and reviewing this collection of information. Send comments regarding this burden estimate or any other aspect of this collection of information, including suggestions for reducing this burden to Department of Defense, Washington Headquarters Services, Directorate for Information Operations and Reports (0704-0188), 1215 Jefferson Davis Highway, Suite 1204, Arlington, VA 22202-4302. Respondents should be aware that notwithstanding any other provision of law, no person shall be subject to any penalty for failing to comply with a collection of information if it does not display a currently valid OMB control number. <b>PLEASE DO NOT RETURN YOUR FORM TO THE ABOVE ADDRESS.</b>					
<b>1. REPORT DATE (DD-MM-YYYY)</b>		<b>2. REPORT TYPE</b>		<b>3. DATES COVERED (From - To)</b>	
<b>4. TITLE AND SUBTITLE</b>				<b>5a. CONTRACT NUMBER</b>	
				<b>5b. GRANT NUMBER</b>	
				<b>5c. PROGRAM ELEMENT NUMBER</b>	
<b>6. AUTHOR(S)</b>				<b>5d. PROJECT NUMBER</b>	
				<b>5e. TASK NUMBER</b>	
				<b>5f. WORK UNIT NUMBER</b>	
<b>7. PERFORMING ORGANIZATION NAME(S) AND ADDRESS(ES)</b>				<b>8. PERFORMING ORGANIZATION REPORT NUMBER</b>	
<b>9. SPONSORING / MONITORING AGENCY NAME(S) AND ADDRESS(ES)</b>				<b>10. SPONSOR/MONITOR'S ACRONYM(S)</b>	
				<b>11. SPONSOR/MONITOR'S REPORT NUMBER(S)</b>	
<b>12. DISTRIBUTION / AVAILABILITY STATEMENT</b>					
<b>13. SUPPLEMENTARY NOTES</b>					
<b>14. ABSTRACT</b>					
<b>15. SUBJECT TERMS</b>					
<b>16. SECURITY CLASSIFICATION OF:</b>			<b>17. LIMITATION OF ABSTRACT</b>	<b>18. NUMBER OF PAGES</b>	<b>19a. NAME OF RESPONSIBLE PERSON</b>
<b>a. REPORT</b>	<b>b. ABSTRACT</b>	<b>c. THIS PAGE</b>			<b>19b. TELEPHONE NUMBER (include area code)</b>

# **Atomic-Scale Factors Guiding the Design of Combustion Nanocatalysts: Structures, Electronic Characteristics and Catalytic Pathways**

## **MURI FINAL REPORT**

**Reporting Period: June 1, 2008 to December 31, 2013**

**March 27, 2014**

**SUBMITTED BY: UZI LANDMAN**  
**([uzi.landman@physics.gatech.edu](mailto:uzi.landman@physics.gatech.edu))**

**MURI - AFOSR Grant No. FA9550-08-1-0323 (Start Date: 01 Jun 2008)**

**PRINCIPAL INVESTIGATOR: Professor Uzi Landman**

**INSTITUTION: School of Physics, Georgia Institute of Technology, Atlanta GA 30332-0430. (Tel: (404) 894-3368).**

**AFOSR PROGRAM MANAGER: Dr. Michael R. Berman, (703) 696-7781,  
[michael.berman@afosr.af.mil](mailto:michael.berman@afosr.af.mil)**

# **Atomic-Scale Factors Guiding the Design of Combustion Nanocatalysts: Structures, Electronic Characteristics and Catalytic Pathways**

## **MURI FINAL REPORT**

**Reporting Period: June 1, 2008 to December 31, 2013**

**MURI - AFOSR Grant No. FA9550-08-1-0323 (Start Date: 01 Jun 2008)**

**PRINCIPAL INVESTIGATOR: Professor Uzi Landman**

**LEAD INSTITUTION: School of Physics, Georgia Institute of Technology, Atlanta GA**

**AFOSR PROG. MANAGER: Dr. Michael R. Berman, (703) 696-7781, michael.berman@afosr.af.mil**

### **PROGRAM OBJECTIVE**

The research program focuses on the development, implementation and use of theoretical methodologies, addressing nanocatalysis issues pertaining to the creation, characterization, atomic-scale manipulations, control and exploitation of nanometer-scale catalytic systems. This research program aims at providing a deep understanding of the physical principles underlying and governing the unique catalytic properties of nanoscale materials to be employed for catalytic combustion of fuels and propellants. Furthermore the research program seeks to establish atomic-scale design principles of individual and integrated nanocatalytic materials systems of basic significance, and of relevance and potential contributions to defense-related missions, industrial processes, and environmental issues.

Some of the key challenges facing the development of combustion catalysts addressed by the research program, include: (i) development of combustion processes occurring at lower temperatures, thus lowering the energy cost as well as reducing the production of hazardous nitrous oxide emissions, (ii) design of catalysts that allow complete fuel combustion in a very short contact time, and (iii) increasing the durability (e.g. against coalescence and sintering) and poison-resistance of combustion catalysts.

The investigations performed in this program are anchored in findings from cluster and surface science studies, pertaining to the atom-by-atom dependencies of energetics, kinetics,

reactivities and catalytic activities of clusters, originating from interplay between size, geometry, dimensionality, and electronic structure, as well as based on extensive experience accumulated over the past several years in studies of oxidation reactions catalyzed by size-selected gas-phase and surface-supported nanostructures. These important objectives and fundamental issues are addressed in the research program through the development and employment of an arsenal of modern first-principles theoretical methodologies of predictive capabilities.

## **SCIENTIFIC APPROACH**

The challenging objectives and fundamental issues that are addressed in this research program pertain to the atom-by-atom dependencies of energetics, kinetics, reactivities and catalytic activities of clusters, originating from an interplay between size, geometry, dimensionality, and electronic structure, on the physical and chemical properties of materials nano-scale materials aggregates.

These questions are approached in our program with the use of an arsenal of modern first-principles theoretical methodologies of predictive capabilities. Our computational methodologies include: (1) First-principles determination of optimal atomic and electronic structures of nanocluster catalyst assemblies (gas-phase and surface-supported nanostructures) and ab-initio molecular dynamics (MD) simulations of catalytic reaction pathways, with the motions of the atoms (or ions) obeying classical equations of motions and the electronic degrees of freedom calculated (self-consistently) concurrent with the instantaneous atomic positions, using the Born-Oppenheimer (BO) spin-density-functional (dynamics (BO-LSD-MD) method developed in our laboratory. (2) Construction and analysis of micro-kinetic models of catalytic reactions, consisting of sets of coupled rate equations. These model calculations assist in the analysis of experiments (particularly gas-phase catalysis in traps) and understanding of the effects of temperature and pressure on the rate of change with time of the concentrations of reactants and products. This information assists us in formulation of catalytic cycles.

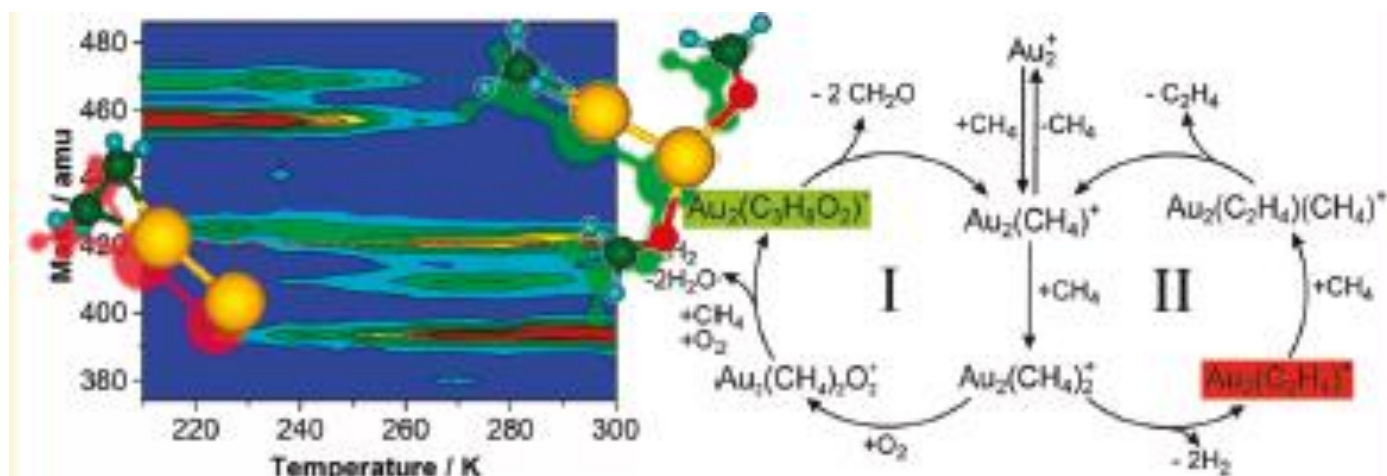
## **SELECTED ACCOMPLISHMENTS DURING THE FIVE YEAR GRANT PERIOD**

Aiming at understanding the catalyzed combustion reaction of the simplest hydrocarbon fuel molecule (methane) with small metal clusters (gold and palladium), quantum calculations of



**(B) PUB 3. The mechanisms of nanocatalytic processes involving methane, CH<sub>4</sub>, leading to the low-temperature production of ethylene, C<sub>2</sub>H<sub>4</sub>, were explored through experiments in a trap (in the multicollision regime) and first-principles theoretical simulations. Detailed microscopic catalytic mechanisms and a catalytic cycle (See Figure above) have been predicted and tested.** For the case of neat methane and gold dimer cations it was found that first each gold atom binds to a methane molecule, and subsequently two hydrogen molecules are eliminated and the two carbon atoms form a double bond. The ethylene precursor binds to one of the gold atom and subsequently another methane molecule binds to the bare Au atom of the dimer, thus lowering the barrier for release of the ethylene product molecule and completing the catalytic cycle. Both the carbon–hydrogen bond activation and the subsequent desorption of the ethylene product molecule require cooperative action of several atoms bound to the gold dimer. Cover article in the Angew. Chem. Int. Ed, 49, 980 (2010)..

**(C) PUB 6. Reaction kinetics and mass spectrometry measured in trap experiments, in conjunction with first-principles density-functional theory simulations, revealed that gold dimer cations catalyze temperature-tuned selective reactions in gaseous mixtures of oxygen and methane (yielding formaldehyde, below 250 K, and ethylene near 300 K).** Temperature-controlled catalytic selectivity was demonstrated through the conversion of a mixture of methane and oxygen to formaldehyde at temperatures below 250K, while at higher temperatures (up to 300K) dehydrogenation processes lead predominantly to formation of ethylene. Microscopic mechanisms (reaction intermediates and transition state configurations and barriers) were predicted theoretically and tested against the measured data. The research appeared as a Cover article of The Journal of Physical Chemistry C, vol 115, p. 6788 (April 14, 2011). This research complemented the joint experimental and theoretical findings, see (B) above, pertaining to the room temperature conversion of ethylene into methane catalyzed by gold dimer cations.



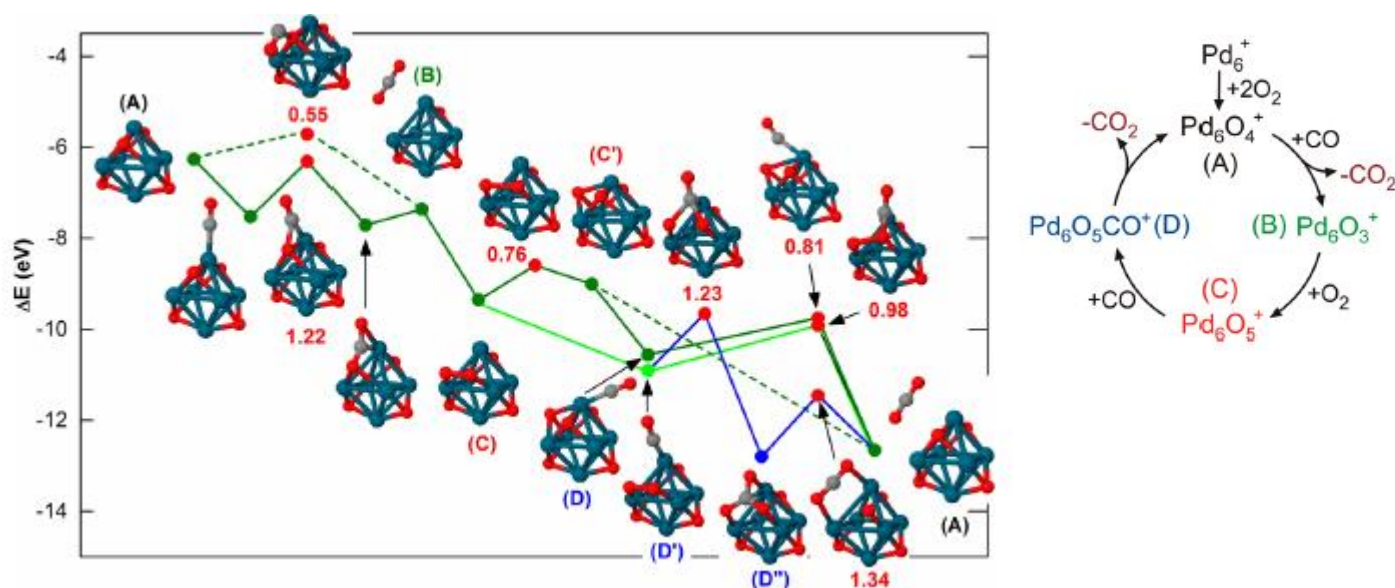
**(D) PUB 11.** The nano-oxide cluster  $\text{Pd}_6\text{O}_4^+$  was identified to be the key intermediate in the catalytic combustion of CO initiated by the oxidation of  $\text{Pd}_6^+$  with molecular oxygen.  $\text{Pd}_6\text{O}_4^+$  contains only dissociated oxygen with each O atom bound to three Pd atoms. Although  $\text{Pd}_6\text{O}_4^+$  appears to be resistant to further oxidation with  $\text{O}_2$ , the chemisorbed atomic oxygen species represent the active oxygen phase for the efficient room temperature catalytic conversion of CO to  $\text{CO}_2$ .

Nanometal oxides are an important class of heterogeneous catalysts for various industrial processes. Several factors are considered as governing the catalytic activity and selectivity of these catalytic materials, including particle size, shape, composition, and, in particular, the chemical nature of the active oxygen species. Consequently, correlations between the oxidation states and catalytic activity are a fundamental topic of investigations pertaining to catalytic activity in general and of oxides in particular.

The palladium oxide cluster  $\text{Pd}_6\text{O}_4^+$  is formed as the sole product upon reaction of a bare palladium cluster  $\text{Pd}_6^+$  with molecular oxygen in an octopole ion trap under multicollision conditions. This oxide cluster is found to be resistant to further oxidation over a large temperature range, and further  $\text{O}_2$  molecules merely physisorb on it at cryogenic temperatures. The particular stability of  $\text{Pd}_6\text{O}_4^+$  is confirmed by the observation that the reaction



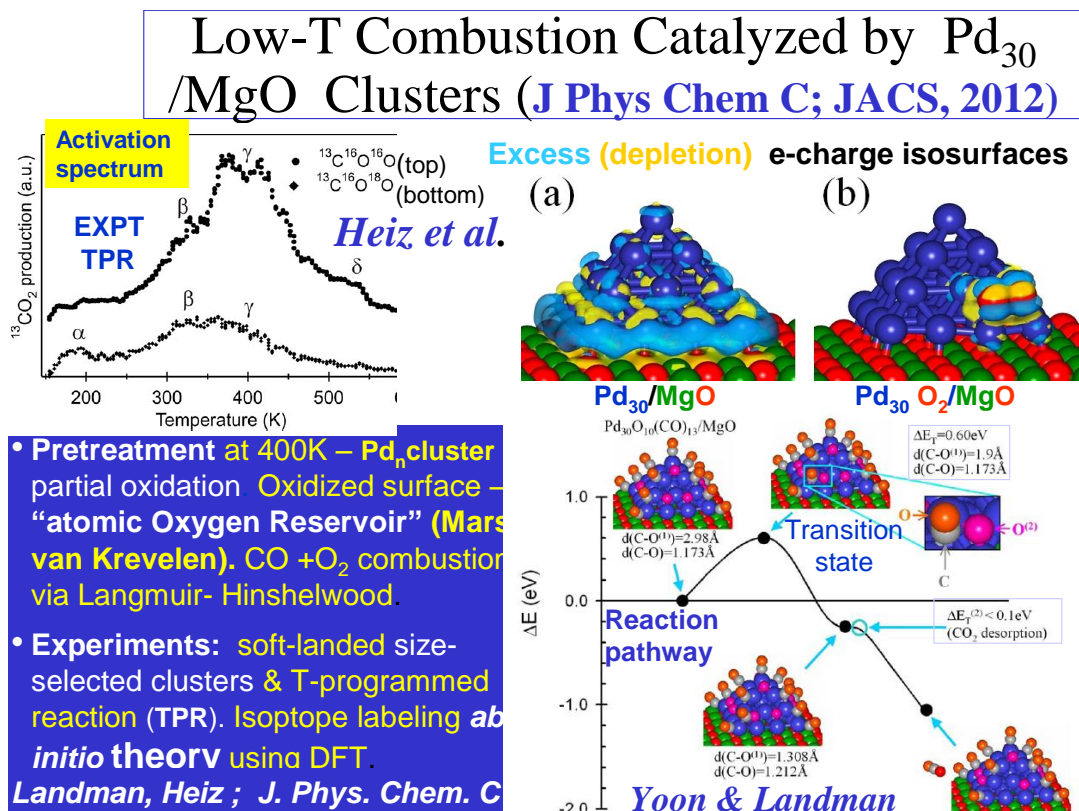
of  $\text{Pd}_7^+$  with  $\text{O}_2$  leads to fragmentation resulting in the formation of  $\text{Pd}_6\text{O}_4^+$ . However, in an oxygen-rich  $\text{O}_2/\text{CO}$  mixture,  $\text{Pd}_6\text{O}_4^+$  is identified as the catalytically active species that effectively facilitates the low-temperature oxidation of CO. Gas-phase reaction kinetics measurements in conjunction with first-principles calculations provide detailed molecular level insight into the nano-oxide cluster chemistry and are able to reveal the full catalytic combustion reaction cycle. These gas-phase results provide information that may be utilized in the design of prospective new nano-oxide-based catalytic materials for low temperature oxidation catalysis.



**(E) PUB 7 & 8. Catalytic oxidation on  $\text{Pd}_n$  nanoclusters (with  $n = 13$  and  $30$ ) supported on a  $\text{MgO}(001)$  surface has been explored with first – principles simulations, in conjunction with experiments (temperature programmed reaction) on supported mass-selected clusters.** The theoretical work addressed issues pertaining to:

- (i) the microscopic mechanisms of the oxidation of up to 30-atom surface-supported Pd clusters serving as CO and methane oxidation catalysts, and
- (ii) the oxidation (combustion) reaction pathways (of CO or methane) via either the van Krevelen mechanism (where the reactant molecules, CO or methane, react with oxygen atoms that are part of a palladium-oxide network

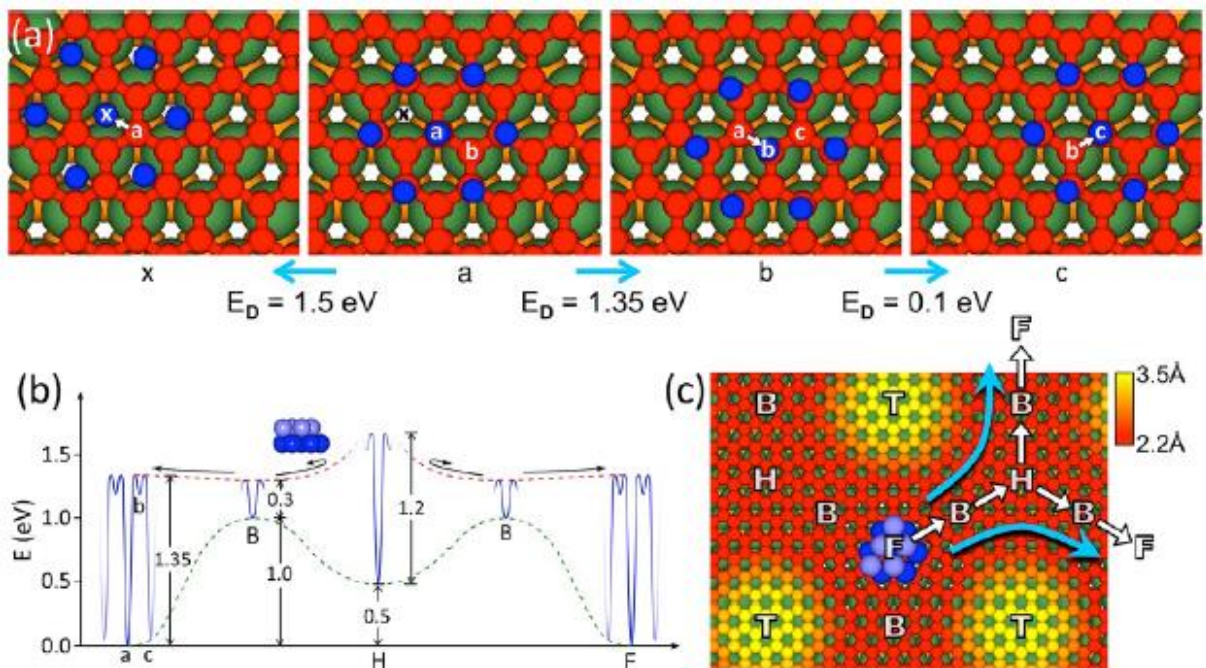
serving as an effective oxygen reservoir), or the Langmuir-Hinshelwood root (where the oxygen and other reactant molecules, e.g. CO or methane, are coadsorbed on the catalyst). The theoretical investigations have shown that catalytic activity of the supported nanoclusters is associated with partially-oxidized of the Pd<sub>n</sub> nanocatalysts, and have elucidated the controlling aspects of structure, reactivity, and activation mechanisms.



**(F) PUB 12. Size-selected monodisperse nanoclusters on supported graphene and their bonding, isomerism, and mobility have been investigated with the use of scanning electron microscopy and first-principles theoretical calculations.** The use of cluster materials in various fields, ranging from optics and electronics to catalysis, brings new opportunities and expands our ability to design and control materials’ functionalities on the atomic scale, owing to the unique chemical and physical properties of these nanostructures. The unique properties of materials’ aggregates with nanoscale dimensions often originate from quantum size effects that emerge at reduced sizes, thus

introducing size (or scale) as an added dimension to the periodic table of the elements. The emerging opportunity of rational design of nanostructured functional materials is based on a deeper understanding of the interplay between morphology and electronic structure as a function of the cluster size. To make progress toward this aim necessitates the development of a methodology that allows a refined degree of monodispersity – a term that we use here in a broadened sense to include not only an absolutely precise selection of particle size, but also an ultrasharp distribution of isomeric form and adsorption (support) environment.

Soft-landing of size-selected  $\text{Pd}_n$  ( $n \leq 20$ ) nano-clusters on a Moiré-patterned surface of graphene adsorbed on Ru(0001), leads to controlled formation of a truly monodisperse cluster-assembled material. Combined scanning tunneling microscopy and first-principles calculations allow identification of self-selective adsorption sites, characterization of size-dependent cluster isomers, and exploration of interconversion processes between isomeric forms that manifestly influence cluster surface mobility. Surface-assembled cluster superstructures may be employed in nanocatalytic applications, as well as in fundamental investigations of physical factors controlling bonding, structure, isomerism, and surface mobilities of surface-supported clusters.

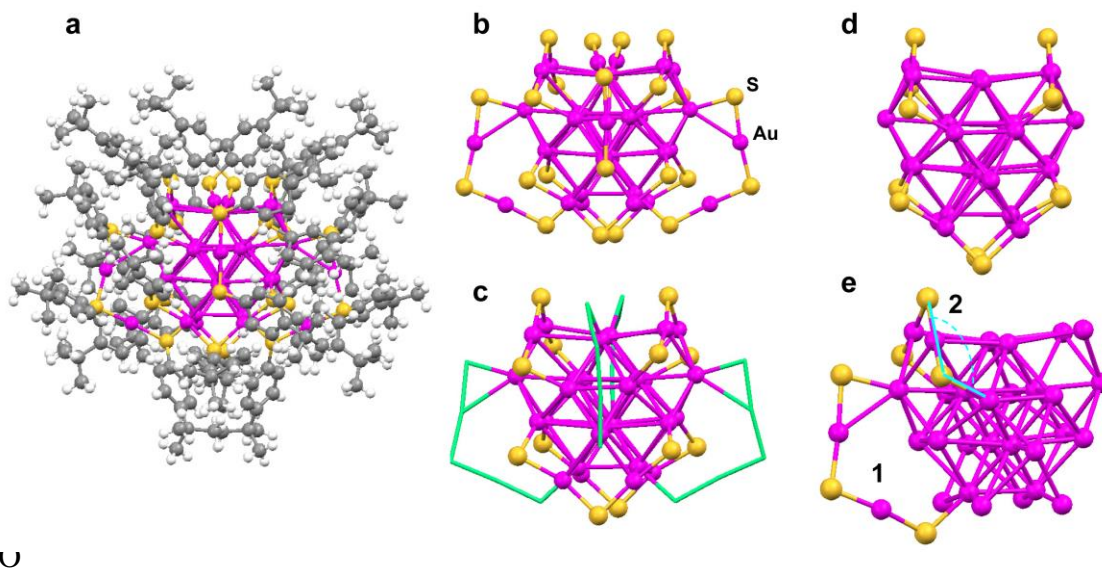


**(G) PUB 9 (also 10, 15, 16). Atomic and Electronic Structure and Stability of Protected Metal Nanocrystalline Clusters.** During the last (option) years of the MURI grant we capitalized on opportunities to resume activities in the field of nanocrystals; we note here that our early activity in this important area of nanoscience -- see our 1996 paper "Nano-Crystal Gold Molecules", W. L. Whetten, J. Khoury, I. Vezmar, S. Murthy, C. L. Cleveland, W. D. Luedtke, U. Landman, *Adv. Mater.* **8**, 428 (1996), that served as a guide and impetus for a large number of subsequent experimental and theoretical efforts world wide. The opportunity to reestablish our leadership position in this field has been coupled to collaborative research with several experimental groups. Here we highlight one of these investigations (Pub. 9), where we collaborated with the experimental group of Prof. Jin (Carnegie Mellon University), where the a total crystal structure determination of a gold nanocrystal consisting of 36 atoms has been determined (adding the fourth known case to the three known structure, being Au<sub>25</sub>, Au<sub>38</sub> and Au<sub>102</sub>), and being the first, x-ray determined gold nanocrystal to exhibit a face-centered-crystal structure.

Gold nanoparticles protected by thiolates, including thiol-terminated DNA and simple thiols, possess extraordinary stability and constitute perhaps the most widely studied system in nanoscience. Understanding and control of the ways that the thiolate ligands protect the underlying gold core and of the atomic structures that the gold cores adopt with decreasing size, are issues of fundamental, and potential practical, importance. For relatively large gold nanoparticles (e.g. > 2 nm), electron microscopy can map out the core structure, but the surface structure (e.g. the ways that thiolates bind to gold) cannot be determined. Obtaining the total structure (i.e. core and surface) necessitates single crystal growth of atomically precise gold nanoparticles. Recently, significant progress has been made in the chemical synthesis of ultrasmall gold nanoparticles (often called nanoclusters, typically < 2nm) protected by thiolates, but the total structure determination of such Au<sub>n</sub>(SR)<sub>m</sub> nanoparticles by X-ray crystallography remains a major challenge. The reported crystal structures thus far include Au<sub>102</sub>(p-MBA)<sub>44</sub>, Au<sub>25</sub>(SCH<sub>2</sub>CH<sub>2</sub>Ph)<sub>18</sub> and Au<sub>38</sub>(SCH<sub>2</sub>CH<sub>2</sub>Ph)<sub>24</sub>, which are all composed of non-FCC (face-centered cubic) kernels, such as the Au<sub>79</sub> decahedron in Au<sub>102</sub>(p-MBA)<sub>44</sub>, the Au<sub>13</sub> icosahedron in Au<sub>25</sub>(SCH<sub>2</sub>CH<sub>2</sub>Ph)<sub>18</sub> and the Au<sub>23</sub> face-sharing bi-icosahedron in Au<sub>38</sub>(SCH<sub>2</sub>CH<sub>2</sub>Ph)<sub>24</sub>. These

experimental examples, as well as theoretical work, indicate a size-dependent general trend that starts from icosahedral atomic arrangements at smaller sizes to decahedral structures at larger ones, and culminating with large clusters of FCC structure (for FCC metals). Pertaining to the surface structures of  $\text{Au}_n(\text{SR})_m$  nanoclusters, unique “staple”-like motifs have been found, including the dimeric staple (i.e.  $-\text{SR}-\text{Au}-\text{SR}-\text{Au}-\text{SR}-$ ) and the monomeric staple (i.e.  $-\text{SR}-\text{Au}-\text{SR}-$ ).

We reported the discovery of a FCC-type core structure in  $\text{Au}_{36}(\text{SR})_{24}$ , where SR refers to 4-*tert*-butylbenzenethiolate (denoted as SPh-Bu<sup>t</sup>). The emergence of FCC structure in  $\text{Au}_{36}(\text{SR})_{24}$  is surprising, given the small size of the cluster. The  $\text{Au}_{36}(\text{SR})_{24}$  particle consists of a  $\text{Au}_{28}$  kernel with a truncated FCC tetrahedron exposing (111) and (100) facets. Unlike the previously reported  $\text{Au}_n(\text{SR})_m$  nanocluster structures ( $n=25, 38, 102$ ), a new type of thiolate binding mode for *all-thiolate*-capped nanoclusters has been discovered, that is, twelve of the 24 ligands bind to the underlying Au atoms in a simple *bridging* mode, with the remaining twelve thiols forming the known dimeric staple motifs.



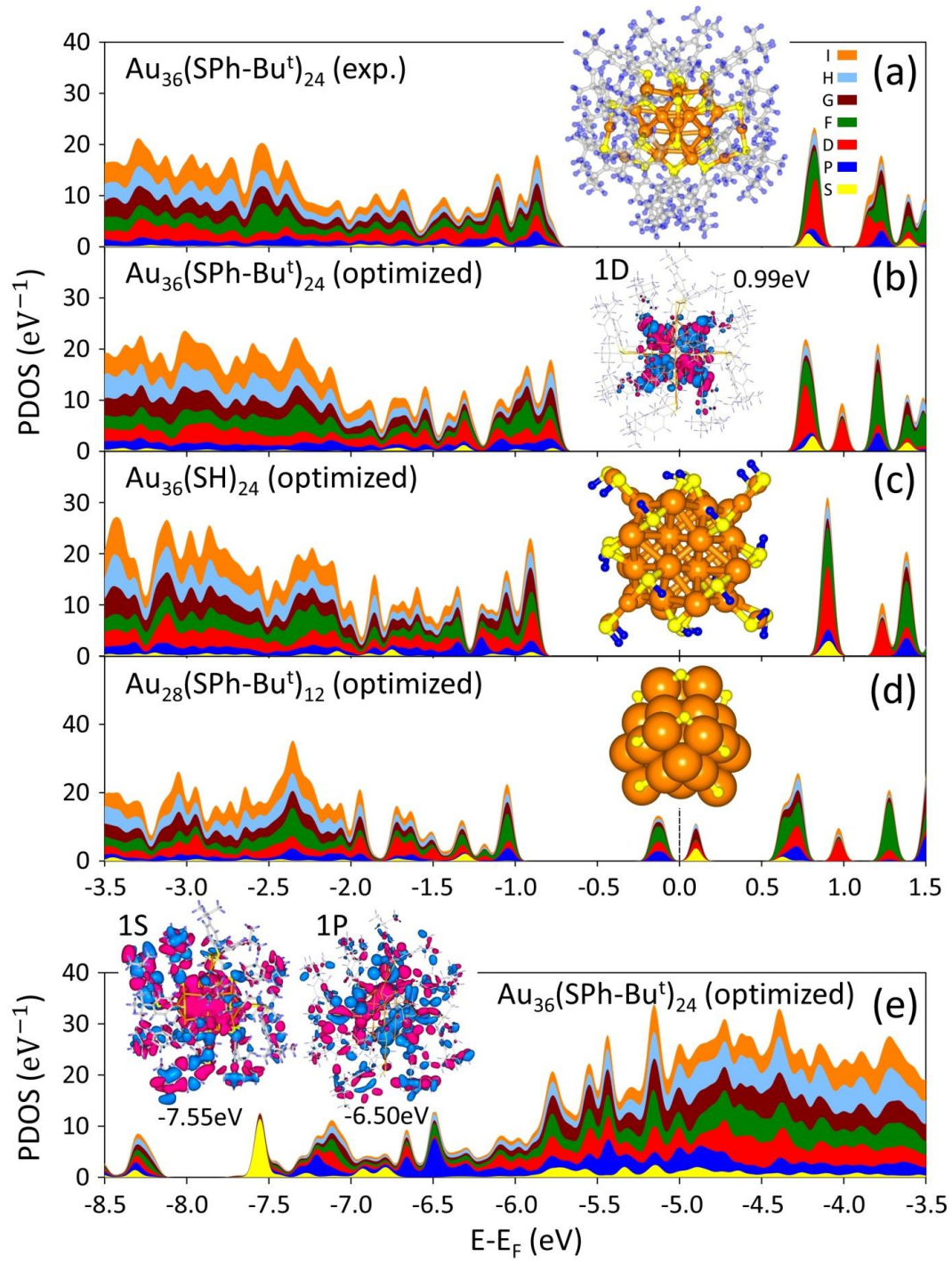
Our first-principles calculations reveal a large energy gap between the highest occupied and lowest unoccupied energy levels ( $\sim 1.7$  eV) in agreement with the measured value by optical absorption spectrum. The high stability of the nanocluster originates from the geometric structure and organization of the electronic states into superatom shells. The new FCC tetrahedral  $\text{Au}_{28}$



kernel and the thiolate bridging mode (as opposed to staple motifs) offer important implications for possible other FCC-structured gold nanocrystals as well as for thiol binding on extended gold surfaces in self-assembled-monolayer (SAM) systems.

To obtain insight into the bonding and electronic structure of the  $\text{Au}_{36}(\text{SR})_{24}$  cluster, we performed extensive first-principles calculations. The figure below displays (in the range  $-3.5 \text{ eV} \leq E - E_F \leq 1.5 \text{ eV}$ ) the projected densities of states (PDOS, see SI for details) calculated for the experimentally determined atomic coordinates (Figure, below, a), for the energy-optimized structure (Figure, below, b), obtained via density-functional-theory (DFT)-based relaxation of the experimental configuration), as well as for the (optimized) structure but with  $R = H$  (Figure, below, c). The first outstanding feature observed is the exceptional large HOMO-LUMO energy gap ( $\Delta_{\text{HL}} = 1.7 \text{ eV}$ ,  $1.5 \text{ eV}$  and  $1.8 \text{ eV}$ , respectively in (a-c in the Figure below). This large gap agrees well with the optically measured one ( $\approx 1.7 \text{ eV}$ ), thus the optical gap represents a true HOMO-LUMO gap. This energy gap exceeds by a large margin those measured for other thiolate-protected gold nanoclusters in this size range, i.e.,  $1.3 \text{ eV}$  for  $\text{Au}_{25}(\text{SR})_{18}$  and  $0.9 \text{ eV}$  for  $\text{Au}_{38}(\text{SR})_{24}$ . As aforementioned, the large  $\Delta_{\text{HL}}$  gap confers high stability to the cluster, endowing it with resistance to chemical attack.

Inspection of the electronic structure of the cluster and the orbitals' angular momentum symmetries shows that, in agreement with our early proposal, while for a wide range of energies (located at the middle of the energy spectrum) the electronic wavefunctions exhibit localized character (associated with Au atomic 5d electrons), the orbitals of states with energies near the top and bottom of the electronic spectra are of delocalized character, derived from the atomic Au 6s electrons (see representative orbital images in b & e in the Figure below). These delocalized states can be assigned particular symmetries following the electronic cluster-shell-model (CSM), with a (superatom) aufbau rule:  $1S^2 | 1P^6 | 1D^{10} | 2S^2 | 1F^{14} | 2P^6 | 1G^{18} | \dots$  where S, P, D, F, and G correspond, respectively, to angular momenta,  $l = 0, 1, 2, 3, 4, \dots$ ; note that the restriction of quantum number  $l = 0, \dots, n-1$  in atoms is not applicable in superatoms. We note here certain possible alterations in level ordering, as well as possible splitting of the  $2l+1$  fold level degeneracy by crystal-field effects. In the above CSM scheme, the vertical lines denote shell-closures (magic numbers), with each closure accompanied by the opening of a stabilizing energy gap. For the  $\text{Au}_{36}(\text{SR})_{24}$  cluster, with the number of electrons not engaged in bonding to sulfur being  $36 - 24 = 12$ , the aufbau rule leads to a  $1S^2 | 1P^6 | 1D^4$  (superatom) configuration, which is not a closed shell one. The stability of this configuration derives instead from the splitting of the 5-fold degeneracy of the 1D shell due to the non-spherical atomic arrangement in the gold cluster and the organization of the protecting ligands. Indeed, this crystal-field-like splitting is mirrored in the observation of three LUMO orbitals of 1D character in the PDOS shown in the Figure, below, b and its inset.



## PUBLICATIONS (Refereed Papers)

1. C. Harding, V. Habibpour, S. Kunz, A. Nam-Su Farnbacher, U. Heiz, B. Yoon and Uzi Landman, "Control and Manipulation of Gold Nanocatalysis: Effects of Metal Oxide Support Thickness and Composition", J. Am. Chem. Soc., **131**, 538 (2009).
2. S.M. Lang, T.M. Bernhardt, R. N. Barnett, B. Yoon, and U. Landman, "Hydrogen-Promoted Oxygen Activation by Free Gold Cluster Cations", J. Am. Chem. Soc., **131**, 8939 (2009).
3. S. M. Lang, T. M. Bernhardt, R.N. Barnett, and U. Landman, "Methane Activation and Catalytic Ethylene Formation on Free  $\text{Au}_2^{++}$ ", Angew. Chem. Int. Ed. **49**, 980 (2010). Cover article.
4. S. M. Lang, T. M. Bernhardt, R. N. Barnett, and U. Landman, "Size-Dependent Binding Energies of Methane to Small Gold Clusters", Chem. Phys. Chem. **11**, 1570 (2010).
5. M. E. Vaida, T. M. Bernhardt, C. Barth, F. Esch, U. Heiz, and U. Landman, "Ultrathin magnesia films as support for molecules and metal clusters: Tuning reactivity by thickness and composition", Physica Status Solidi B **247**, No. 5, 1001 (2010).
6. S. M. Lang, T. M. Bernhardt, R. N. Barnett, and U. Landman, "Temperature-Tunable Selective Methane Catalysis on  $\text{Au}_2^+$ : From Cryogenic Partial Oxidation Yielding Formaldehyde to Cold Ethylene Production", J. Phys. Chem. C, **115**, 6788 (2011). Cover article.
7. B.Yoon, U.Landman, V.Habibpour, C. Harding, S. Kunz, U. Heiz, M. Moseler, M. Walter "Oxidation of Magnesia-Supported  $\text{Pd}_{30}$  Nanoclusters and Catalyzed CO Combustion: Size-Selected Experiments and First-Principles Theory", J. Phys. Chem. C, **116**, 9594 (2012) .



8. M. Moseler, M. Walter, B. Yoon, U. Landman, V. Habibpour, C. Harding, S. Kunz, and U. Heiz “Oxidation State and Symmetry of Magnesia-Supported Pd<sub>13</sub>O<sub>x</sub> Nanocatalysts Influence Activation Barriers of CO Oxidation”, J. Am. Chem. Soc. **134**, 7690 (2012).
9. C. Zeng, H. Qian, T. Li, G. Li, N. L. Rosi, B. Yoon, R. N. Barnett, R. L. Whetten, U. Landman, and R. Jin “Total Structure of the Golden Nanocrystal Au<sub>36</sub>(SR)<sub>24</sub>”, Angew. Chem. Int Ed. **51**, 13114 (2012).
10. I. Chakraborty, A. Govindarajan, J. Erusappan, A. Ghosh, T. Pradeep, B. Yoon, R. L. Whetten, and U. Landman “The Superstable 25-*kDa* Monolayer Protected Silver Nanoparticle: Measurements and Interpretation as an Icosahedral Ag<sub>152</sub>(SCH<sub>2</sub>CH<sub>2</sub>Ph)<sub>60</sub> Cluster, Nano Letters **12** (11), 5861–5866 (2012).
11. S. M. Lang, I. Fleischer, T. M. Bernhardt, R. N. Barnett, U. Landman. “Pd<sub>6</sub>O<sub>4</sub><sup>+</sup>: An oxidation resistant yet highly catalytically active nano-oxide cluster”, J. Am. Chem. Soc. **134**, 20654 (2012).
12. B. Wang, B. Yoon, M. König, Y. Fukamori, F. Esch, U. Heiz, U. Landman “Size-selected monodisperse nano-clusters on supported graphene: Isomerism and mobility”, Nano Letters **12** (11), 5907–5912 (2012).
13. P. Nimmala, R. L. Whetten, A. Dass, B. Yoon, U. Landman, “Au<sub>67</sub>(SR)<sub>35</sub> Nanomolecules: Synthesis, Isolation, Characterization and First-Principles Theoretical Analysis”, J. Phys. Chem. A **117**, 504 (2013).
14. “Oxidative thymine mutation in DNA: Water-wire-mediated proton-coupled electron transfer”, R. N. Barnett, J. Joseph, U. Landman, G. B. Schuster, J. Am. Chem. Soc. **135**, 3904 (2013).
15. D. Bahena, N. Bhattarai, U. Santiago, A. Tlahuice, A. Ponce, S. B. H. Bach, B. Yoon, R. L. Whetten, U. Landman, M. J-Yacaman, “STEM Electron Diffraction and High-

Resolution Images Used in the Determination of the Crystal Structure of the  $\text{Au}_{144}(\text{SR})_{60}$  Cluster”, J. Phys. Chem. Lett. **4**, 975 (2013).

- 16.** A. Baksi, T. Pradeep, B. Yoon, C. Yannouleas, U. Landman, “Bare clusters derived from protein templates:  $\text{Au}_{25}^{+}$ ,  $\text{Au}_{38}^{+}$  and  $\text{Au}_{102}^{+}$ ”, ChemPhysChem **14**, 1272 (2013).

## **PREENTATIONS (Uzi Landman)**

Plenary Lecture, Conference on Challenges in Catalysis, University of California, Santa Barbara, August (2008).

Plenary Lecture, Internatioal Symposium on Powders and Inorganic Clusters (ISSPIC 14), Valladolid, Spain, September(2008).

Invited Lecture, Physics of Clusters and Nanomaterials, Allahabad, India, February (2009).

Plenary Lecture, S3C conference on size selected clusters, Brand Austria, March (2009).

Plenary Speaker, TNT09, Trends in Nanotechnology, Barcelona, Spain, September (2009).

Invited Speaker, Nanostructures at Surfaces, Monte Verita, Switzerland, September (2009).

Invited Speaker, Symposium on “Advances in Nanoscience”, San Sebastian, Spain, November (2009).

Plenary Speaker, ICONSAT (Intenational Conference on Nano Science & Technology, Mumbai, India, February (2010).

Invited Speaker, TNT-2010, Trends in Nanotechnology, Braga Portugal, September, 2010.

The S. Lifson Annual Memorial Lecture, Weizmann Institute of Science, Rehovot, Israel, February, 2011

Kriedel Memorial Lecture, 23<sup>rd</sup> Annual Rio Grande Symposium on Advanced Materials, Albuquerque, NM, October 2011.

Invited Speaker, NanoScience Days, Jyvaskyla, Finland, October, 2011

Keynote Lecture, TNT-2011, Tenerife, Canary Islands, November, 2011.

Invited Lecture, AFOSR Review of Catalytic Nanocombustion, Salt Lake City, December, 2011.

Plenary Lecture, Iconsat 2012 (International Conference on nanoscience and Technology), Hydrabad, India January, 2012.

Invited speaker, Functional Clusters, Genesis Foundation Symposium, Nagoya, Japan, February, 2012.

Key note Lecture, NanoIsrael 2012, Tel Aviv, Israel, March, 2012.

Invited Lecture, MRS annual meeting, San Francisco, CA, April, 2012

Invited Lecture, AFOSR Molecular Dynamics Program Review, Washington DC, May, 2012.

U. Landman

Invited Lecture, ISSPIC 16, Leuven, Belgium, July , 2012.

Invited Lecture, ACS, Philadelphia, PA, August, 2012.

Keynote Lecture, Trends in Nanotechnology (TNT2012), Madrid, Spain, September, 2012.  
Keynote Lecture, TRAIN2 International Conference, Barcelona, Spain, November, 2012.  
Invited Lecture, AFOSR MURI meeting, Low-Temperature Combustion, Atlanta, GA, December, 2012.  
Plenary Lecture S3C, Conference on Frontiers in Clusters, Davos, Switzerland, March , 2013.  
Keynote Lecture, Gordon Research Conference, August , 2013.

## **RESEARCHERS SUPPORTED BY THE MURI GRANT**

Dr. Bokwon Yoon – Research Scientist II  
Dr. Robert N. Barnett – Senior Research Scientist  
Dr. Jianping Gao – Senior Research Scientist

## **MOST RECENT GOVERNMENT REVIEWS & RELATED MEETINGS**

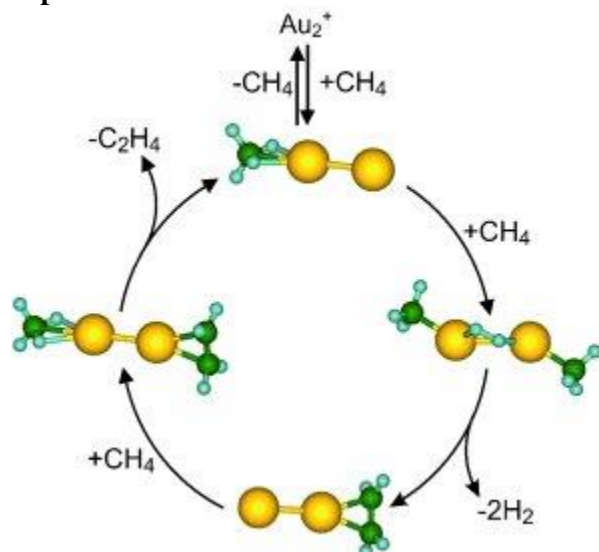
June 2008 – Washington DC, AFOSR MURI Kickoff Meeting, U. Landman.  
May 2009 – San Diego, AFOSR Contactors Meeting, Molecular Dynamics, U. Landman  
December 2009 – Washington DC, AFOSR MURI Review, U. Landman and R.N. Barnett  
July 2010 – Washington DC, DoD MURI Conference, U. Landman  
December 2011 – Yale University, New Haven, AFOSR MURI Review, U. Landman  
December 2012 – Georgia Institute of Technology, Atlanta , GA, AFOSR , MURI Researchers meeting.

## PRESS RELEASES ABOUT WORK PUBLISHED UNDER THIS GRANT

### Catalytic Dimers of Gold Atoms Make Ethylene from Methane

Published on **January 19, 2010** at 5:16 AM

Ethylene is a primary feedstock for chemical industry, and particularly for the production of plastics like polyethylene and polystyrene. Ethylene is currently made by the steam cracking of fossil fuel fractions. A possible alternative to this may be the production of ethylene from methane, because although fossil fuel supplies are slowly declining, methane is still found in giant natural gas deposits.



© Wiley-VCH

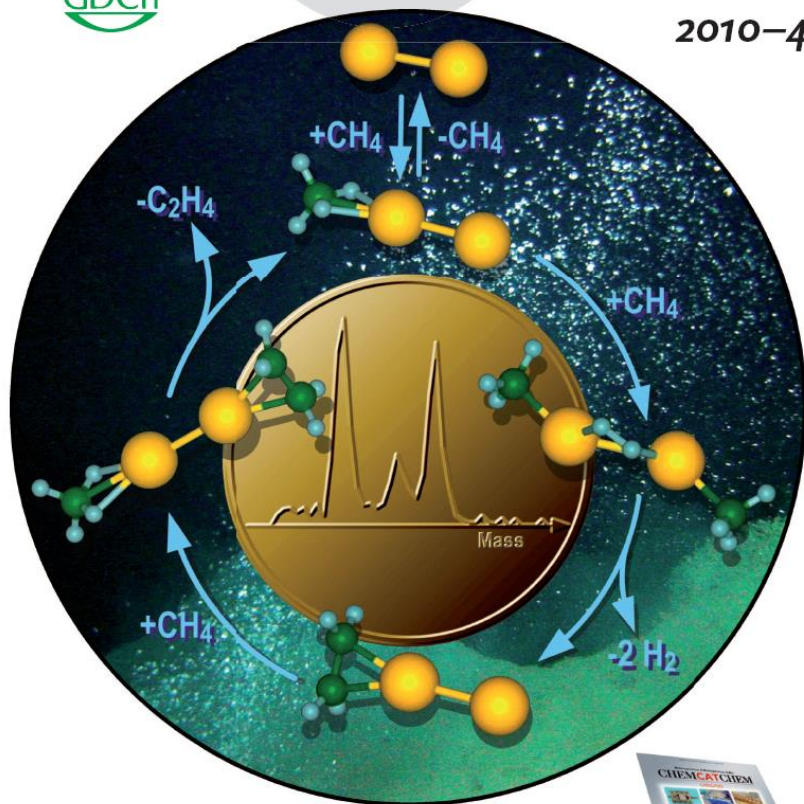
The problem is that the carbon–hydrogen bonds in methane are very difficult to break. It thus usually takes extreme conditions to induce the carbon in methane to form bonds with other carbon atoms. Furthermore, this reaction usually produces a mixture. Scientists working with Thorsten M. Bernhardt at the University of Ulm (Germany) and Uzi Landman at the Georgia Institute of Technology (Atlanta, USA), have now found a process by which methane can be selectively converted into ethylene at low pressures and temperatures. Free gold dimers catalyze the reaction, the researchers report in the journal [Angewandte Chemie](#).

“Methane activation, meaning the ‘cracking’ of C–H bonds, is a very complex process,” explain the scientists, “which must be understood at the molecular level before practically applicable catalytic processes can be developed.” To investigate this, the team carried out experiments with

different catalytic metal clusters (aggregates of a few metal atoms) as model systems. In tests with particles made of a few gold atoms, they found that positively charged particles made of two gold atoms ( $\text{Au}_2^+$ ) selectively convert methane into ethylene in the gas phase.

Through experiments in which intermediates of the reaction were “trapped”, as well as model computations, the researchers were able to formulate a reaction mechanism for this catalytic cycle. Each gold atom of the gold dimers binds to a methane molecule; hydrogen is split off and the two carbon atoms form a single bond to each other. This ethylene precursor initially remains bound to one of the gold atoms, and the freed gold atom binds to a new methane molecule. In the last step, another methane molecule displaces the ethylene precursor from its spot on the gold atom and ethylene is released. At this point the reaction cycle can begin again.

“Both the activation of the carbon–hydrogen bonds of the methane and the subsequent splitting off of the ethylene molecule require cooperative action of several atoms bound to the gold dimer,” Bernhardt and Landman explain further details of the mechanism. “Our insights are not only of fundamental interest, but may also be of practical use.”



**Nanoprobes**

M. Orrit et al.

**Organocatalysis**

B. Westermann et al.

**Methane Activation**

D. Schröder



WILEY-VCH

ACIEFS 49 (5) 821–988 (2010) · ISSN 1433–7851 · Vol. 49 · No. 5

## Scientists Finely Control Methane Combustion to Get Different Products

Posted **April 14, 2011** Atlanta, GA

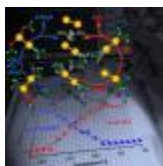
### For More Information Contact

David Terraso

Communications and Marketing

404-385-2966

### Related Media



#### Controlling Methane Combustion to Get Different Products

Scientists have discovered a method to control the gas-phase selective catalytic combustion of methane, so finely that if done at room temperature the reaction produces ethylene, while at lower temperatures it yields formaldehyde. The process involves using gold dimer cations as catalysts — that is, positively charged diatomic gold clusters. Being able to catalyze these reactions, at or below room temperature, may lead to significant cost savings in the synthesis of plastics, synthetic fuels and other materials. The research was conducted by scientists at the Georgia Institute of Technology and the University of Ulm. It appears in the April 14, 2011, edition of *The Journal of Physical Chemistry C*.

“The beauty of this process is that it allows us to selectively control the products of this catalytic system, so that if one wishes to create formaldehyde, and potentially methyl alcohol, one burns methane by tuning its reaction with oxygen to run at lower temperatures, but if it’s ethylene one is after, the reaction can be tuned to run at room temperature,” said Uzi Landman, Regents’ and Institute Professor of Physics and director of the Center for Computational Materials Science at Georgia Tech.

Reporting last year in the journal *Angewandte Chemie International Edition*, a team that included theorists Landman and Robert Barnett from Georgia Tech and experimentalists Thorsten Bernhardt and Sandra Lang from the University of Ulm, found that by using gold dimer cations as catalysts, they can convert methane into ethylene at room temperature.



This time around, the team has discovered that, by using the same gas-phase gold dimer cation catalyst, methane partially combusts to produce formaldehyde at temperatures below 250 Kelvin or -9 degrees Fahrenheit. What's more, in both the room temperature reaction-producing ethylene, and the formaldehyde generation colder reaction, the gold dimer catalyst is freed at the end of the reaction, thus enabling the catalytic cycle to repeat again and again.

The temperature-tuned catalyzed methane partial combustion process involves activating the methane carbon-to-hydrogen bond to react with molecular oxygen. In the first step of the reaction process, methane and oxygen molecules coadsorb on the gold dimer cation at low temperature. Subsequently, water is released and the remaining oxygen atom binds with the methane molecule to form formaldehyde. If done at higher temperatures, the oxygen molecule comes off the gold catalyst, and the adsorbed methane molecules combine to form ethylene through the elimination of hydrogen molecules.

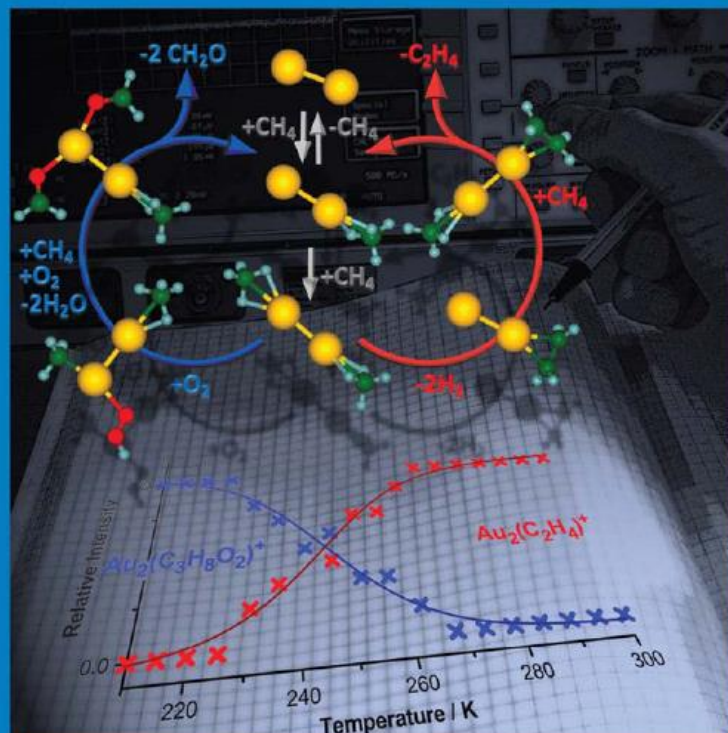
In both the current work, as well as in the earlier one, Bernhardt's team at Ulm conducted experiments using a radio-frequency trap, which allows temperature-controlled measurement of the reaction products under conditions that simulate realistic catalytic reactor environment. Landman's team at Georgia Tech performed first-principles quantum mechanical simulations, which predicted the mechanisms of the catalyzed reactions and allowed a consistent interpretation of the experimental observations.

In future work, the two research groups plan to explore the use of multi-functional alloy cluster catalysts in low temperature-controlled catalytic generation of synthetic fuels and selective partial combustion reactions.

APRIL 14, 2011  
VOLUME 115  
NUMBER 14  
[pubs.acs.org/JPCCE](http://pubs.acs.org/JPCCE)

# THE JOURNAL OF PHYSICAL CHEMISTRY

C



NANOMATERIALS, INTERFACES, HARD MATTER



ACS Publications  
MOST TRUSTED. MOST CITED. MOST READ.

[www.acs.org](http://www.acs.org)

## CAPTION

Low- (blue) and high- (red) temperature  $\text{Au}_2^+$ -catalyzed methane activation selective reaction cycles. Reaction kinetics and mass spectrometry radio frequency trap experiments in conjunction with first-principles density functional theory simulations reveal that gold dimer cations catalyze temperature-tuned selective reactions in gaseous mixtures of oxygen and methane. Temperature-controlled catalytic selectivity is demonstrated through the conversion of a mixture of methane and oxygen to formaldehyde at temperatures below 250 K (left catalytic cycle, blue color), while at higher temperatures (up to 300 K) dehydrogenation processes lead predominantly to formation of ethylene (right catalytic cycle, red color). On the bottom chart, we display the measured relative intensities of the catalyzed reaction products plotted versus the reaction temperature. Microscopic mechanisms were predicted theoretically and tested against the measured data. The corresponding molecular structures of the reaction intermediates and products are superimposed on the reaction cycles. Gold atoms are depicted by yellow spheres, oxygen atoms are in red, carbon atoms are in green, and hydrogen atoms are described by small blue spheres. See page 6788. [View the article.](#)

**In the following we reproduce a Commentary published at the invitation of the Editor-in-Chief of Angewandte Chemie regarding the publication of our paper:**

**“Methane Activation and Catalytic Ethylene Formation on Free  $\text{Au}_2^+$ ”, S. M. Lang, T. M. Bernhardt, R.N. Barnett, and U. Landman, Angew. Chem. Int. Ed. 49, 980 (2010).**

# Activation of Methane by Gaseous Metal Ions\*\*

Detlef Schröder\*

C–C coupling · C–H activation · gas-phase reactions · metal ions · methane

Methane is one of the most ubiquitous feedstocks available in large amounts from petrological as well as biogenic resources. Its economic use for purposes other than mere combustion remains a conceptual problem, however. Steam reforming converts methane into syngas [Eq. (1)] from which methanol can be produced in a second step [Eq. (2)]; the CO:H<sub>2</sub> ratio of the syngas can be adjusted by the water–gas-shift reaction.<sup>[1]</sup> While the technology of this process is well developed, investment volumes are large and smaller sources of methane cannot be exploited this way.



Considerable research efforts are devoted to alternative routes and a particularly attractive variant would be the selective partial oxidation of methane according to Equation (3). Methanol as a liquid, easily transportable, and chemically versatile product offers several advantages and it has even been suggested as the basis of future energy economy.<sup>[2]</sup> While easily written on paper, Equation (3) poses quite a formidable challenge, because methane is the least reactive of all hydrocarbons and hence needs a highly reactive catalyst for activation, whereas methanol can easily be oxidized further, ultimately leading to complete combustion. The selective functionalization of methane has accordingly received quite some attention in condensed-phase research and several promising systems have been developed,<sup>[3]</sup> though they are still far away from practical applications.<sup>[4]</sup>



An alternative approach to achieve a fundamental understanding into the requirements for the C–H bond activation of methane are model studies of small reactive fragments in the gas phase.<sup>[5,6]</sup> In this area, interesting progress has been achieved recently. In 2006 it was reported that methane could be activated by MgO<sup>+</sup>, the first main-group metal oxide

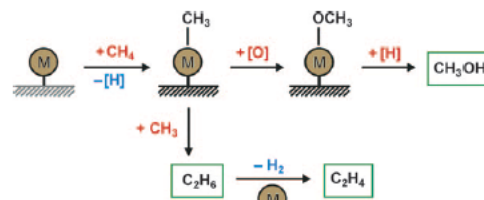
cation to do this,<sup>[7]</sup> and by V<sub>4</sub>O<sub>10</sub><sup>+</sup>, the first metal oxide cluster.<sup>[8]</sup> Shortly afterwards (Al<sub>2</sub>O<sub>3</sub>)<sub>n</sub><sup>+</sup> (n = 3–5) was reported as the first oxide clusters of a main-group metal to activate methane;<sup>[9]</sup> also methane activations by non-metallic elements have been found more recently.<sup>[10]</sup> Most of these reactions are driven by the radicaloid nature of the oxide cations with the spin mostly located on oxygen, which leads to a high preference for hydrogen-atom abstraction from methane to generate methyl radicals. This situation is in contrast to the dehydrogenation of methane by various 5d elements to give metal carbenes MCH<sub>2</sub><sup>+</sup>,<sup>[6,11]</sup> or MCH<sub>2</sub><sup>2+</sup>,<sup>[6,12]</sup> and to the C–C coupling reactions with methane observed for medium-sized hydrocarbon dications,<sup>[13]</sup> in which the dehydrogenation takes place with the “CH<sub>2</sub>” fragment remaining at the ionic species.

To date, nearly all the bare metal cations M<sup>+</sup> have been screened experimentally with respect to their reactivity towards methane.<sup>[6,14]</sup> Bare metal cations are, however, an extreme simplification in comparison to real catalysts and in this respect the investigation of gaseous metal clusters is of prime interest.<sup>[15]</sup> While platinum clusters in various charge states have been shown to activate methane,<sup>[16,17]</sup> to date, gold clusters, like most other M<sub>n</sub><sup>+/–</sup> ions, were considered to be unreactive towards methane.<sup>[18]</sup>

The C–H bond activation of methane is, however, only the first step. The second task is to selectively convert the (free or bound) methyl radical into useful products (Scheme 1), for example, through the C–O coupling with a suitable oxidant to afford methanol [Eq. (3)]. Alternatively, C–C coupling of two methyl entities can lead to ethane which may then be converted into the basic chemical ethene [Eq. (4)].



In this respect, Lang et al. report in this issue that isolated Au<sub>2</sub><sup>+</sup> cluster cations can mediate a C–C coupling of methane



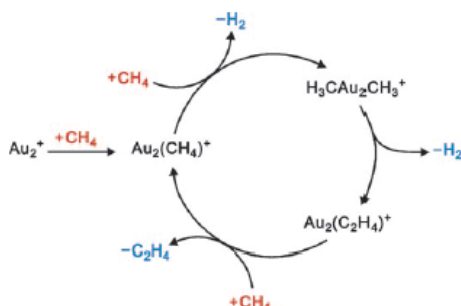
**Scheme 1.** C–H bond activation of methane and subsequent C–O or C–C coupling.

[\*] Dr. D. Schröder  
Institute of Organic Chemistry and Biochemistry, Academy of Sciences of the Czech Republic  
Flemingovo náměstí 2, 16610 Prague 6 (Czech Republic)  
E-mail: schroeder@uochb.cas.cz

[\*\*] This work was supported by the Academy of Sciences of the Czech Republic (Z40550506) and the European Research Council (AdG HORIZOMS).



to afford ethene.<sup>[19]</sup> To this end, they used an ion trap, which—simply put—is the gas-phase chemist's equivalent of a chemical reactor. Specifically, mass-selected  $\text{Au}_2^+$  ions (approximately  $10^6$  ions) were trapped for hundreds of milliseconds in  $\text{CH}_4/\text{He}$  mixtures at pressures of about 1 Pa and temperatures between 200 and 300 K. By careful investigation of the reaction kinetics and the effects of temperature in combination with an exhaustive theoretical study, a catalytic cycle for the dehydrogenative coupling of methane to give ethene could be established (Scheme 2). In addition to the phenomenological description of the processes observed, Lang et al. quantitatively modeled the observed product distribution and thereby derived essential thermodynamic and kinetic parameters.



**Scheme 2.** Simplified representation of the catalytic cycle for the C–C coupling of methane to ethene realized by Lang et al.<sup>[19]</sup>

Several aspects of this work are remarkable:

- 1) Unlike most other gas-phase studies, relatively high pressures are applied, that is, a multicolisional regime is explored which enables the stabilization of reaction intermediates as well as the occurrence of endothermic reactions at increased reaction times.
- 2) The results illustrate a methane coupling occurring at ambient temperatures, and the analysis of kinetic profiles as a function of temperature provides deep mechanistic insight including the estimation of activation energies.
- 3) In the multicolisional mechanism, methane plays a crucial role not only as the reactant, but also as a ligand which can replace the product ethene associated to the  $\text{Au}_2^+$  species.

These aspects are of particular relevance with regard to the so-called pressure gap,<sup>[20]</sup> which often hampers the translation of model studies to real catalysis. In their recent work, Lang et al. indeed manage to bridge this gap at least partially. Their study may thus be considered as an important step in basic research towards the understanding of catalytic cycles, which may also bear practical relevance.

Received: November 19, 2009

[1] J.-P. Lange, *Catal. Today* **2001**, *64*, 3–8.

[2] G. A. Olah, A. Goepfert, G. K. S. Prakash, *Beyond Oil and Gas: The Methanol Economy*, Wiley-VCH, Weinheim, **2006**.

- [3] a) R. A. Periana, D. J. Taube, S. Gamble, H. Taube, T. Satoh, H. Fujii, *Science* **1998**, *280*, 560–564; b) J. A. Labinger, J. E. Bercaw, *Nature* **2002**, *417*, 507–514; c) M. Lersch, M. Tilset, *Chem. Rev.* **2005**, *105*, 2471–2526.
- [4] J. A. Labinger, *J. Mol. Catal. A* **2004**, *220*, 27–35.
- [5] D. K. Böhme, H. Schwarz, *Angew. Chem.* **2005**, *117*, 2388–2406; *Angew. Chem. Int. Ed.* **2005**, *44*, 2336–2354.
- [6] For methane and small alkanes, see: a) D. Schröder, H. Schwarz, *Proc. Natl. Acad. Sci. USA* **2008**, *105*, 18114–18119; b) M. Schlangen, H. Schwarz, *Dalton Trans.* **2009**, 10155–10165; c) J. Roithová, D. Schröder, *Chem. Rev.* **2010**, *110*, DOI: 10.1021/cr900183p.
- [7] a) D. Schröder, J. Roithová, *Angew. Chem.* **2006**, *118*, 5835–5838; *Angew. Chem. Int. Ed.* **2006**, *45*, 5705–5708. See also: b) A. Bozovic, D. K. Bohme, *Phys. Chem. Chem. Phys.* **2009**, *11*, 5940–5951.
- [8] S. Feyel, J. Döbler, D. Schröder, J. Sauer, H. Schwarz, *Angew. Chem.* **2006**, *118*, 4797–4801; *Angew. Chem. Int. Ed.* **2006**, *45*, 4681–4685.
- [9] S. Feyel, J. Döbler, R. Hockendorf, M. K. Beyer, J. Sauer, H. Schwarz, *Angew. Chem.* **2008**, *120*, 1972–1976; *Angew. Chem. Int. Ed.* **2008**, *47*, 1946–1950.
- [10] a)  $\text{BF}_2^+$ : F. Pepi, A. Tata, S. Garzoli, M. Rosi, *Chem. Phys. Lett.* **2008**, *461*, 21–27; b)  $\text{P}_4\text{O}_{10}^+$ : N. Dietl, M. Engesser, H. Schwarz, *Angew. Chem.* **2009**, *121*, 4955–4957; *Angew. Chem. Int. Ed.* **2009**, *48*, 4861–4863; c)  $\text{SO}_2^+$ : G. de Petris, A. Troiani, M. Rosi, G. Angelini, O. Ursini, *Chem. Eur. J.* **2009**, *15*, 4248–4252; d)  $\text{As}^+$ ,  $\text{Se}^+$ : X. Zhang, H. Schwarz, *Chem. Eur. J.* **2009**, *15*, 11559–11565.
- [11] K. K. Irikura, J. L. Beauchamp, *J. Am. Chem. Soc.* **1991**, *113*, 2769–2770.
- [12] L. G. Parke, C. S. Hinton, P. B. Armentrout, *J. Phys. Chem. A* **2008**, *112*, 10469–10480, and references therein.
- [13] a) C. L. Ricketts, D. Schröder, C. Alcaraz, J. Roithová, *Chem. Eur. J.* **2008**, *14*, 4779–4783; b) J. Roithová, C. L. Ricketts, D. Schröder, *Int. J. Mass Spectrom.* **2009**, *280*, 32–37.
- [14] A. Shayesteh, V. V. Lavrov, G. K. Koyanagi, D. K. Bohme, *J. Phys. Chem. A* **2009**, *113*, 5602–5611.
- [15] a) G. E. Johnson, E. Tyo, A. W. Castleman, Jr., *Proc. Natl. Acad. Sci.* **2008**, *105*, 18108–18113; b) G. E. Johnson, R. Mitric, V. Bonačić-Koutecký, A. W. Castleman, Jr., *Chem. Phys. Lett.* **2009**, *475*, 1–9.
- [16]  $\text{Pt}_n^+$ : a) U. Achatz, C. Berg, S. Joos, B. S. Fox, M. K. Beyer, G. Niedner-Schatteburg, V. E. Bondybey, *Chem. Phys. Lett.* **2000**, *320*, 53–58; b) C. Adlhart, E. Uggerud, *Chem. Commun.* **2006**, 2581–2582;  $\text{Pt}_n^0$ : c) D. J. Trevor, D. M. Cox, A. Kaldor, *J. Am. Chem. Soc.* **1990**, *112*, 3742–3749;  $\text{Pt}_n^+$ : d) T. Hamura, M. Ichibashi, T. Kondow, *J. Phys. Chem. A* **2002**, *106*, 11465–11469; e) K. Koszinowski, D. Schröder, H. Schwarz, *J. Phys. Chem. A* **2003**, *107*, 4999–5006; f) G. Kummerlöwe, I. Balteanu, Z. Sun, O. P. Balaj, V. E. Bondybey, M. K. Beyer, *Int. J. Mass Spectrom.* **2006**, *254*, 183–188; g) C. Adlhart, E. Uggerud, *Chem. Eur. J.* **2007**, *13*, 6883–6890.
- [17] a) D. M. Cox, R. Brickman, K. Creegan, A. Kaldor, *Z. Phys. D* **1991**, *19*, 353–355; b) K. Koszinowski, D. Schröder, H. Schwarz, *ChemPhysChem* **2003**, *4*, 1233–1237; c) S. M. Lang, T. M. Bernhardt, *Eur. Phys. J. D* **2009**, *52*, 139–142.
- [18] For the spectacular effect of a single argon ligand on the activation of methane by  $\text{Rh}_2^+$ , see: G. Albert, C. Berg, M. Beyer, U. Achatz, S. Joos, G. Niedner-Schatteburg, V. E. Bondybey, *Chem. Phys. Lett.* **1997**, *268*, 235–241.
- [19] S. M. Lang, T. M. Bernhardt, R. M. Barnett, U. Landman, *Angew. Chem.* **2010**, *122*, 993–996; *Angew. Chem. Int. Ed.* **2010**, *49*, 980–983.
- [20] R. Imbihl, R. J. Behm, R. Schlögl, *Phys. Chem. Chem. Phys.* **2007**, *9*, 3459.